Article

Correlation between C=O Stretching Vibrational Frequency and pK$_a$ Shift of Carboxylic Acids

Keisuke Saito,* Tianyang Xu, and Hiroshi Ishikita*

Read Online

ACCESS | Metrics & More | Article Recommendations | Supporting Information

ABSTRACT: Identifying the pK$_a$ values of aspartic acid (Asp) and glutamic acid (Glu) in active sites is essential for understanding enzyme reaction mechanisms. In this study, we investigated the correlation between the C=O stretching vibrational frequency ($\nu_{C=O}$) of protonated carboxylic acids and the pK$_a$ values using density functional theory calculations. In unsaturated carboxylic acids (e.g., benzoic acid analogues), $\nu_{C=O}$ decreases as the pK$_a$ increases (the negative correlation), whereas in saturated carboxylic acids (e.g., acetic acid analogues, Asp, and Glu), $\nu_{C=O}$ increases as the pK$_a$ increases (the positive correlation) as long as the structure of the H-bond network around the acid is identical. The negative/positive correlation between $\nu_{C=O}$ and pK$_a$ can be rationalized by the presence or absence of the C=C double bond. The pK$_a$ shift was estimated from the $\nu_{C=O}$ shift of Asp and Glu in proteins on the basis of the negative correlation derived from benzoic acids. The previous estimations should be revisited by using the positive correlation derived in this study, as demonstrated by quantum mechanical/molecular mechanical calculations of $\nu_{C=O}$ and electrostatic calculations of pK$_a$ on a key Asp85 in the proton-transfer pathway of bacteriorhodopsin.
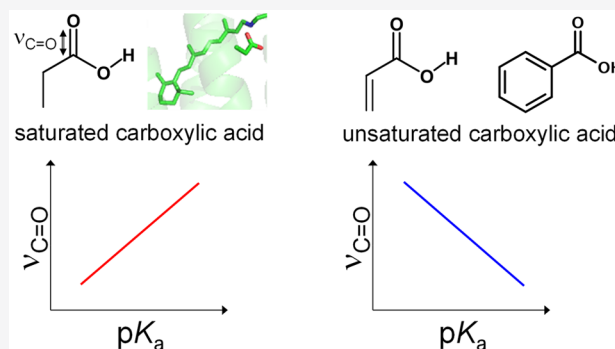
INTRODUCTION

The carboxylic groups (COOH) of aspartic acid (Asp) and glutamic acid (Glu) in proteins play crucial roles especially in proton-transfer pathways[1−6], as their protonation/deprotonation states can be altered due to pK$_a$ shifts caused by interactions with surrounding protein environments.[5,7] Vibrational spectroscopy using infrared light [e.g., Fourier transform infrared spectroscopy (FTIR)] can be used for identifying the protonation state of carboxylic acids.[8] The stretching vibrational frequency, $\nu_{C=O}$, indicates the protonation state of the carboxylic group (i.e., 1690−1750 cm^{-1} for COOH, and 1540−1650 and ~1300−1420 cm^{-1} for the asymmetric and symmetric stretching modes of COO^{-}, respectively) (Figure 1a).[9]

$\nu_{C=O}$ of COOH in proteins can be an indicator of the pK$_a$ shifts of Asp and Glu in active sites because pK$_a$ and $\nu_{C=O}$ are affected by the surrounding (protein) environment. Infrared spectroscopy using benzoic acid analogues[8,10] showed a negative correlation between the pK$_a$ and $\nu_{C=O}$, in which $\nu_{C=O}$ decreased as the pK$_a$ increased (Figure 1b). On the basis of this negative correlation, the observed values of $\nu_{C=O}$ have been discussed in relation to the pK$_a$ of carboxylic acids.[11,12]

A light-driven proton-pumping membrane protein, bacteriorhodopsin, shows different $\nu_{C=O}$ values for the same protonated Asp. Bacteriorhodopsin displays a proton-pumping function across the membrane as a cyclic reaction that comprises a series of intermediates, designated as the J, K, L,

M, N, N′, and O states (see the Results and Discussion for details).[13,14] Proton pumping involves a chromophore (the retinal Schiff base) and a key Asp residue (Asp85) located in the interior. An FTIR study showed that the $\nu_{C=O}$ value of Asp85 is 1761 cm^{-1} in the M intermediate state, whereas it is 1754 cm^{-1} in the N intermediate state, which is a decrease of 7 cm^{-1} from the M state.[11,15] Braiman et al. speculated that Asp85 in the N state (1754 cm^{-1}) would have a higher pK$_a$ than that in the M state (1761 cm^{-1})[11] on the basis of the negative correlation between the $\nu_{C=O}$ and pK$_a$ derived from benzoic acids.[8,10] However, pK$_a$(Asp85) must decrease during the transition from the M to N states becuase of the following reason. The retinal Schiff base is deprotonated in the M state, whereas it is protonated in the N state. Therefore, protonated Asp85 could be unstable because of a repulsive Coulombic interaction with the protonated retinal Schiff base in the N state,[11] resulting in a decrease in pK$_a$(Asp85). A decrease in pK$_a$(Asp85) is plausible because it facilitates proton transfer from Asp85 during the subsequent transition from the final
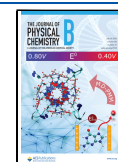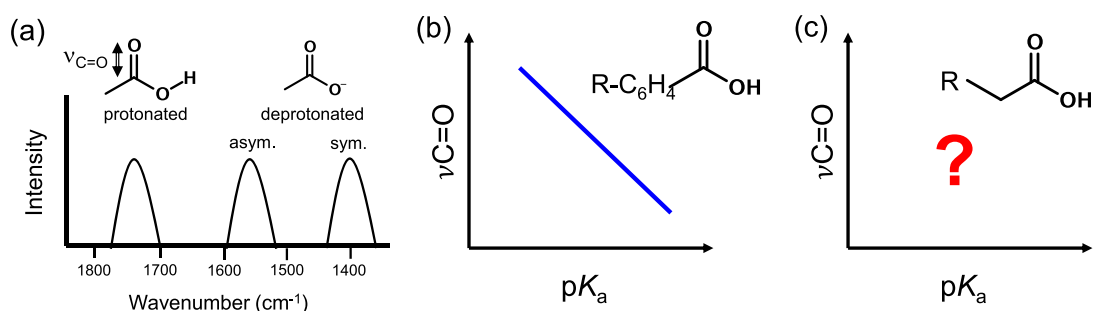
Figure 1. (a) $\nu_{C=O}$ of protonated (COOH) and deprotonated (COO$^-$) carboxylic acids. COO$^-$ has the high-frequency asymmetric (asym) and the low-frequency symmetric (sym) stretching modes. (b) Observed correlation between $\nu_{C=O}$ and pK_a in benzoic acids. (c) Relationship between $\nu_{C=O}$ and pK_a in saturated acids. It was notreported.
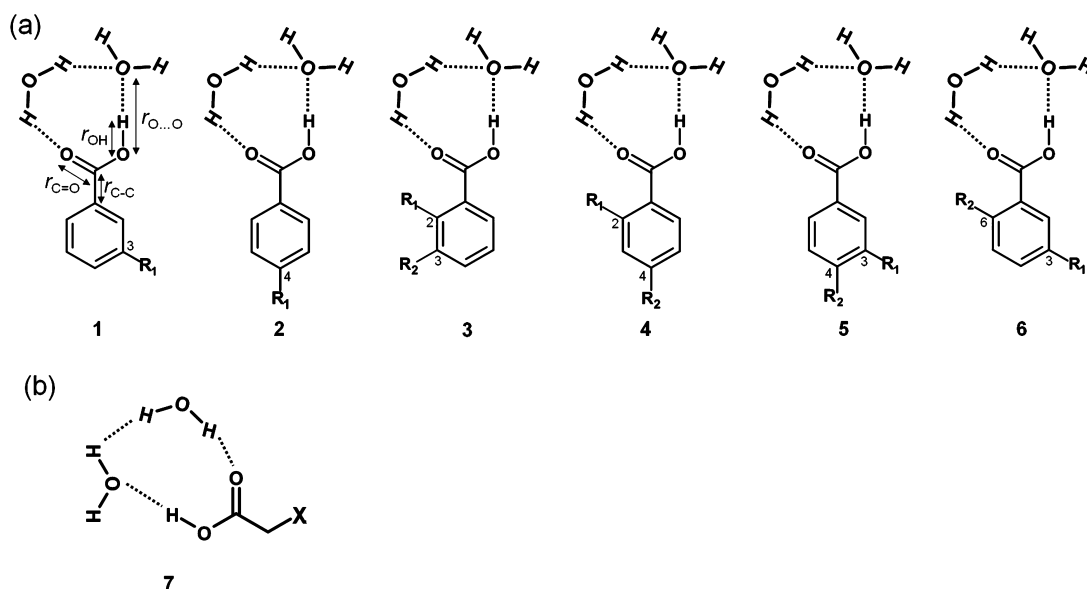

Figure 2. Chemical structure of (a) benzoic acid analogues and (b) acetic acid analogues with distances $r_{C=O}$, r_{OO}, and r_{OH}. The benzoic acid analogues are shown so that the H- bond structue is idencital. The proton was placed at the distal oxygen atom from the substituent group at the ortho position (i.e., the higher-frequency[20] form).

intermediate O state to the initial state (BR) after the N state. Thus, the higher pK_a(Asp85) in the N state estimated from $\nu_{C=O}$ is not consistent with the reaction mechanism of bacteriorhodopsin.

For deprotonated saturated carboxylic acids (COO$^-$), a correlation between the asymmetric vibrational frequency and pK_a was reported; the frequency increased as pK_a decreased.[9,16] For protonated saturated carboxylic acids (COOH), the relationship between $\nu_{C=O}$ and H-bond structures was reported; $\nu_{C=O}$ decreased as the number of H-bonds increased.[17−19] However, to the best of our knowledge, the correlation between $\nu_{C=O}$ and pK_a remains unclear (Figure 1c), particularly for Asp and Glu (i.e., saturated carboxylic acids). In this study, we investigated the correlation between these parameters for both unsaturated carboxylic acids (e.g., benzoic acids) and saturated carboxylic acids (e.g., acetic acids). We also calculated the pK_a value by using an electrostatic-potential approach and the $\nu_{C=O}$ value of Asp85 in bacteriorhodopsin by using a quantum mechanical/molecular mechanical (QM/MM) approach.

■ **METHODS**

Geometry Optimization. To investigate the vibrational frequencies of the isolated carboxylic acids, the protonated carboxylic acid and two adjacent water molecules accepting the H-bond from the OH of the carboxylic group and donating the H-bond to C=O were modeled (Figure 2). These geometries were optimized by using the restricted density functional theory (DFT) method with the B3LYP functional and the 6-31g* basis set, which was performed by using the Jaguar program code.[21]

The atomic coordinates of bacteriorhodopsin were taken from the X-ray structures from *Halobacterium salinarum* for the M state at a resolution of 1.52 Å (PDB code, 1P8H)[22] and the N′ state (V49A mutant) at a resolution of 1.62 Å (PDB code, 1P8U).[22] The N′ state was used as a model structure of the N state of the wild type Results and Discussion. The atomic partial charges of the amino acids and Schiff base were adopted from the all-atom CHARMM22 parameter set.[23] The Schiff base was considered protonated except in the M state. The electrostatic embedding QM/MM scheme was used, wherein the electrostatic and steric effects created by the protein environment were explicitly considered. To perform the QM/MM calculation, we used the QSite[24] program code, employing the restricted DFT method with the B3LYP functional and the 6-31g* basis set. The QM region comprised the side chain of Lys216 (Schiff base), the retinal and side chain of Asp85, Tyr57, and Asp212, and the adjacent water

molecules (W603, W604, and W605 in 1IW9 and W401, W406 and W407 in 1P8U). The coordinates of the heavy atoms in the surrounding MM region were fixed at their original X-ray coordinates, whereas those of the H atoms in the MM region were optimized by using the OPLS2005 force field. All atomic coordinates in the QM region were fully relaxed (i.e., not fixed) in the QM/MM calculation.

Vibrational Frequency Calculation. Vibrational frequencies were calculated by using the same level of theory as the geometry optimizations based on the quantum-chemically optimized structures. The calculated frequencies were scaled by using a standard factor of 0.9614 for B3LYP.[25]

pK_a Calculation of Bacteriorhodopsin Asp85. The computation was based on the electrostatic continuum model by solving the linear Poisson−Boltzmann equation using the MEAD program.[26] To obtain the absolute pK_a value of Asp85, we calculated the difference in electrostatic energy between the protonated and deprotonated states in a reference model system by using a known experimentally measured pK_a value (e.g., 4.0 for Asp[27]). The difference in the pK_a value of the protein relative to the reference system was added to the known reference pK_a value. The experimentally measured pK_a values used as references were 7.2 for the Schiff base,[28,29] 12.0 for Arg, 4.0 for Asp, 9.5 for Cys, 4.4 for Glu, 10.4 for Lys, 9.6 for Tyr,[27] and 7.0 and 6.6 for the Nε and Nδ atoms of His, respectively.[30−32] All other titratable sites were fully equilibrated to the protonation state of the target site during titration. The dielectric constants were set to 4 and 80 for the protein and water, respectively. All computations were performed at 300 K, pH 7.0, and an ionic strength of 100 mM using the QM/MM-optimized structures. The linear Poisson−Boltzmann equation was solved by using a three-step grid-focusing procedure at resolutions of 2.5, 1.0, and 0.3 Å. The ensemble of protonation patterns was sampled by using the Monte Carlo method with Karlsberg.[33] Monte Carlo sampling yielded the probabilities of the two protonation states (protonated and deprotonated) of the molecule. On the basis of the Henderson−Hasselbalch equation, the pK_a value was obtained as the bias potential when the probabilities of the protonated and deprotonated states were 0.5.

■ RESULTS AND DISCUSSION

Benzoic and Acetic Acids. The vibrational frequencies of the C=O stretching bond, $\nu_{C=O}$, were investigated for a series of protonated benzoic acid analogues (Table 1 and Figure 2a) and acetic acid analogues (Table 2 and Figure 2b). In benzoic acids, the calculated $\nu_{C=O}$ negatively correlates with the measured pK_a value (Figure 3a),[10] which is consistent with the infrared spectroscopy results (Figure 3b).[8,10] In contrast, the calculated $\nu_{C=O}$ positively correlates with the measured pK_a value[34] in acetic acids (Figure 3c). A similar positive correlation between the calculated $\nu_{C=O}$ and the measured pK_a was also observed for hydroxycarboxylic acid analogues (Table S1, Figures S1 and S2).

As pK_a increases, the C=O bond distance ($r_{C=O}$; Figure 2a) increases in benzoic acids (Figure 4a). On the other hand, it decreases in acetic acids as pK_a increases (Figure 4c). In benzoic acids, the distance of the C−C bond (r_{C-C}; Figure 2a) connecting the benzene ring to the carboxylic group also correlates with the measured pK_a value (Figure 4b). The calculations for various H-bond structures show that $\nu_{C=O}$ decreases as the number of H-bonds increases (Figure S3), as previously reported.[17−19]

Table 1. Series of Analogues of Benzoic Acid[a]

name	structure[b]	R$_1$[b]	R$_2$[b]	pK_a[c]
3-bromobenzoic acid	1	Br	-	3.85
3-hydroxybenzoic acid	1	OH	-	4.14
3-aminobenzoic acid	1	NH$_2$	-	4.40
3-methylbenzoic acid	1	CH$_3$	-	4.31
4-bromobenzoic acid	2	Br	-	4.01
4-aminobenzoic acid	2	NH$_2$	-	4.90
4-methylbenzoic acid	2	CH$_3$	-	4.40
3-methyl-4-chloro-benzoic acid	5	CH$_3$	Cl	4.07
3-methyl −4-bromo-benzoic acid	5	CH$_3$	Br	4.03
3-chloro-4-methylbenzoic acid	5	Cl	CH$_3$	4.06
3-bromo-4-methylbenzoic acid	5	Br	CH$_3$	3.96
2-chloro-3-methylbenzoic acid	3	Cl	CH$_3$	3.00
2-bromo-3-methylbenzoic acid	3	Br	CH$_3$	3.90
2-methoxy-3-methylbenzoic acid	3	OCH$_3$	CH$_3$	3.84
2-chloro-4-methylbenzoic acid	4	Cl	CH$_3$	3.27
2-bromo-4-methylbenzoic acid	4	Br	CH$_3$	3.09
3-methyl-6-chlorobenzoic acid	6	Cl	CH$_3$	3.12
3-methyl-6-bromobenzoic acid	6	Br	CH$_3$	3.00
3-nitrobenzoic acid	1	NO$_2$	-	3.53
4-nitrobenzoic acid	2	NO$_2$	-	3.46
2-nitro-3-methylbenzoic acid	3	NO$_2$	CH$_3$	2.91
3-methyl-4-nitrobenzoic acid	5	NO$_2$	CH$_3$	3.65
3-nitro-4-methylbenzoic acid	5	CH$_3$	NO$_2$	3.62
3-methyl-6-nitrobenzoic acid	6	NO$_2$	CH$_3$	2.55
2-nitro-4-methylbenzoic acid	4	NO$_2$	CH$_3$	2.68

[a]A previous experimental study reported that these compounds showed a negative correlation between pK_a and $\nu_{C=O}$.[8,10] [b]See Figure 2a. [c]Reference 10.

Table 2. Series of Analogues of Acetic Acid

name	structure[a]	X[a]	pK_a[b]
bromoacetic acid	7	Br	2.86
iodoacetic acid	7	I	3.12
chloroacetic acid	7	Cl	2.86
fluoroacetic acid	7	F	2.66
acetic acid	7	H	4.76

[a]See Figure 2b. [b]Reference 34.

In both benzoic acids and acetic acids, the O−H distance of the protonated carboxylic group (r_{OH}; Figure 2) increases as pK_a decreases (Figure S4c,d). The same trend has been reported in a DFT study of chlorophenols.[35] This is because as pK_a decreases, the deprotonation is facilitated and the proton departs from the donor O atom; thus, r_{OH} increases. In addition, the H-bond distance between the oxygen atoms of the carboxylic acid and the water molecule, $r_{O...O}$ (Figure 2), decreases as pK_a decreases in both cases (Figure S4a,b). This is because the H-bond distance tends to shorten as the pK_a difference between the donor (carboxylic group) and acceptor (water molecule) moieties approaches zero,[36] forming a low-barrier hydrogen bond (LBHB).

The correlation between $r_{C=O}$ and pK_a in acetic acids (Figure 3c) is opposite to that observed for benzoic acids (Figure 3a) because of the opposite correlations between r_{OH} and $r_{C=O}$ [positive for acetic acids (Figures 4c and S4d) and negative for benzoic acids (Figures 4a and S4c)]. Because $\nu_{C=O}$ is determined by the C=O bond strength, $\nu_{C=O}$ increases as $r_{C=O}$ decreases (being a stronger C=O bond),
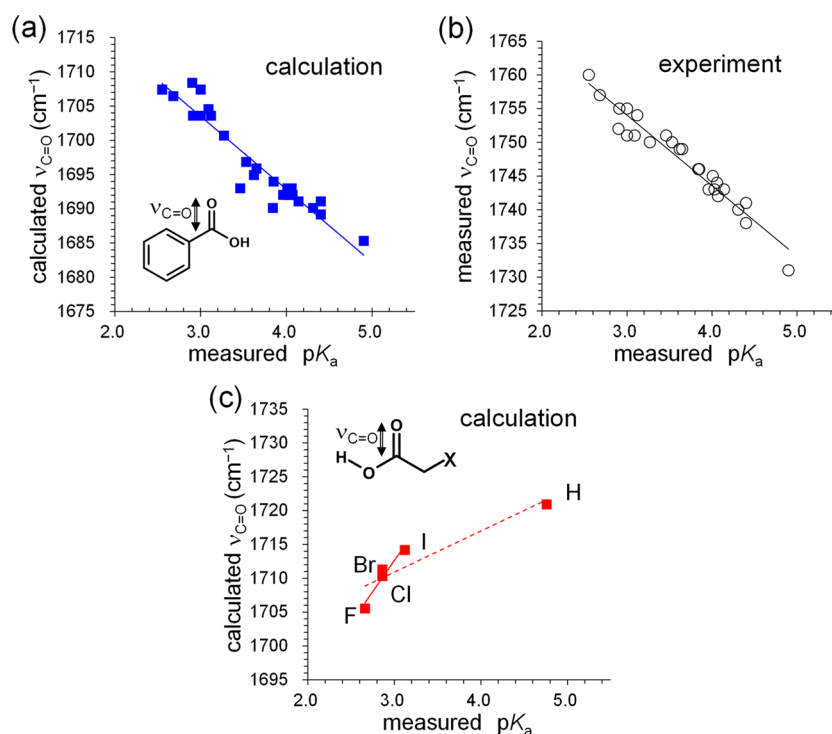
Figure 3. Correlation between the measured pK_a and $\nu_{C=O}$. (a) Calculated $\nu_{C=O}$ of benzoic acids shown in Table 1 and Figure 2a. The determination coefficient R^2 is 0.91. (b) Measured $\nu_{C=O}$ of benzoic acids.[10] R^2 is 0.94. (c) Calculated $\nu_{C=O}$ of acetic acids shown in Table 3 and Figure 2b. R^2 is 0.84. The solid line indicates the fitting line for F, Br, Cl, and I ($R^2 = 0.92$). The dotted line indicates the fitting line for F, Br, Cl, I, and H for comparison ($R^2 = 0.85$).
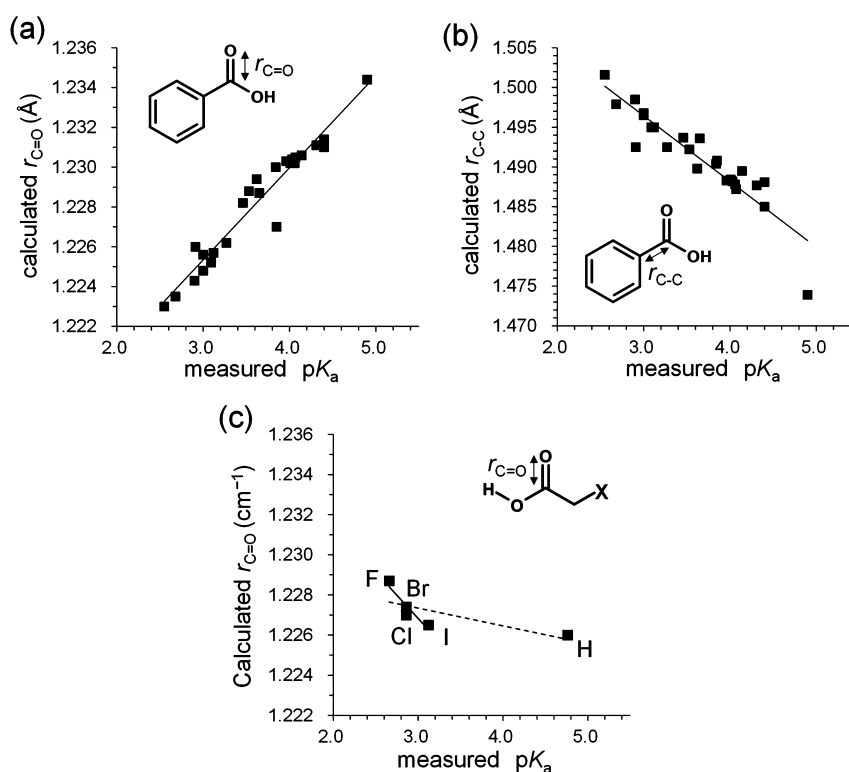

Figure 4. Correlation between the measured pK_a and the calculated distances. (a) C=O bond distance ($r_{C=O}$) of benzoic acids. R^2 is 0.93. (b) C–C bond distance (r_{C-C}) of benzoic acids. R^2 is 0.84. (c) C=O bond distances ($r_{C=O}$) of acetic acids. The solid line indicates the fitting line for F, Br, Cl, and I for comparison ($R^2 = 0.86$). The dotted line indicates the fitting line for F, Br, Cl, I, and H for comparison ($R^2 = 0.54$).

thus corroborating the results of a previous DFT study on carboxylic acids.[18]

The positive and negative correlations between r_{OH} and $r_{C=O}$ in acetic acids and benzoic acids can be explained by the
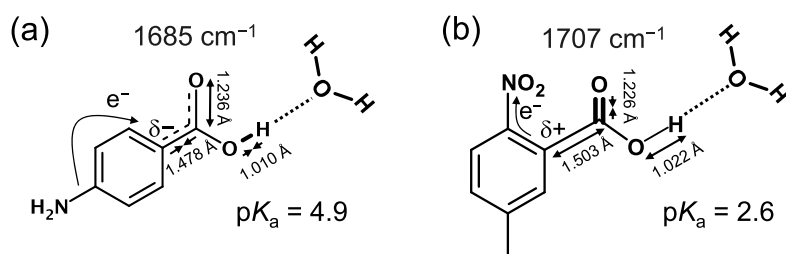
Figure 5. Correlation between r_{OH} and $r_{C=O}$ in benzoic acids. (a) 4-Aminobenzoic acid with $pK_a = 4.9$.[10] (b) 2-Methyl-6-nitrobenzoic acid with $pK_a = 2.6$.[10] The calculated values of $\nu_{C=O}$, r_{OH}, $r_{C=O}$, and r_{C-C} are shown.

presence or absence of a C=C double bond (Figures 5 and 6). Acetic acids have no C=C bonds conjugated with the

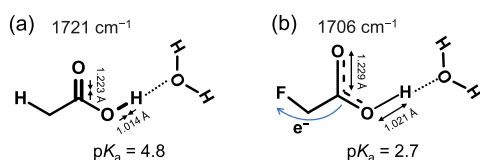**Figure 6.** Correlation between r_{OH} and $r_{C=O}$ in acetic acids. (a) Acetic acid with $pK_a = 4.8$.[34] (b) Fluoroacetic acid with $pK_a = 2.7$.[34] The calculated values of $\nu_{C=O}$, r_{OH}, and $r_{C=O}$ are shown.

carboxylic group (Figure 6). In this case, as the proton leaves the donor O atom, the resonance effect between the C=O and C−O bonds in the carboxylic group becomes more pronounced, which weakens the double-bond nature of the C=O bond. Thereafter, the C=O bond strength is weakened, resulting in a longer $r_{C=O}$ than the typical C=O bond distance (Figure 6b). In contrast, benzoic acids have a C=C bond on the phenyl group conjugated with the carboxylic group (Figure 5). When benzoic acids have an electron-donating substituent (e.g., NH_2), the excess electrons are localized on the benzene ring (Figure 5a). As the deprotonated carboxylic group is destabilized by repulsive interactions with these excess electrons, pK_a increases. Simultaneously, the C−C bond connecting the carboxylic group to the benzene ring has a partial double-bond structure. The bond alternation effect between the C−C and C=O bonds becomes less pronounced, thereby weakening the C=O bond strength, resulting in a long C=O distance ($r_{C=O}$). When benzoic acid has an electron-accepting substituent (e.g., NO_2), the substituent extracts an electron, yielding a positive partial charge on the benzene ring (Figure 5b). As the deprotonated carboxylic group is stabilized by attractive interactions with the positive partial charge, pK_a decreases. Simultaneously, the C−C bond connecting the carboxylic group to the benzene ring has a single-bond nature exclusively, resulting in a longer r_{C-C} (Figure 5b). The bond alternation effect becomes more pronounced and strengthens the C=O bond, resulting in a short C=O distance ($r_{C=O}$). Thus, aspartic acids and benzoic acids show positive and negative correlations, respectively, between r_{OH} and $r_{C=O}$ and between pK_a and $\nu_{C=O}$.

Bacteriorhodopsin. We investigated the correlation between $\nu_{C=O}$ and pK_a in proteins using bacteriorhodopsin for the following reasons: (i) the protonation and deprotonation of Asp are essential in the proton pump function of bacteriorhodopsin, (ii) considerable knowledge of its vibrational spectra from FTIR studies has been accumulated, (iii) the protein structures of the intermediate states have been

repoted, and (iv) the pK_a values of key residues have been reported.

In bacteriorhodopsin, the proton pump function involves four protonatable sites: aspartic acid Asp96 on the cytoplasmic side, Asp85 and the retinal Schiff base in the middle region of the transmembrane helices, and pairing of Glu194 and Glu204 on the extracellular side (Figure 7a). In the initial BR state,
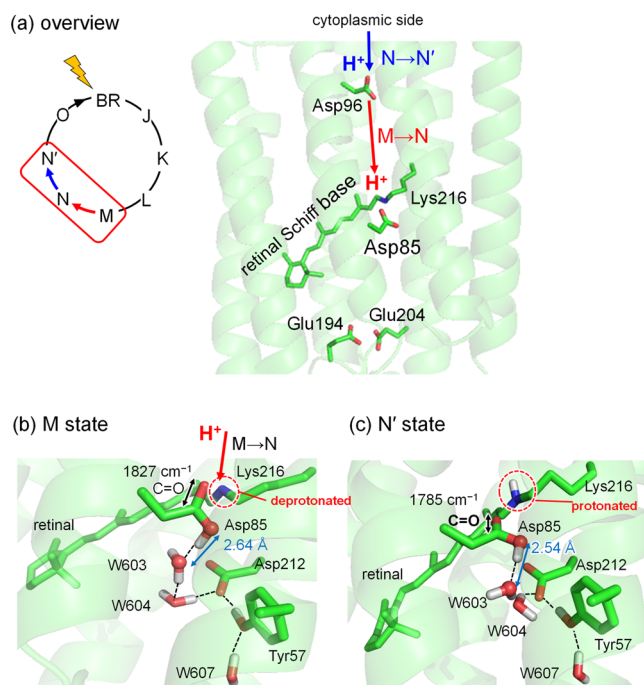

Figure 7. Structure of bacteriorhodopsin. (a) Intermediate states in the cyclic reaction and titratable sites involving the proton pump function in bacteriorhodopsin. The light enegy induces the first transiton from the initial BR state to the J intermediate state. The proton transfer from Asp96 to the retinal Schiff base bonded to Lys216 (red arrow) occurs during the transition from the M to N states. The proton transfer from the cytoplasmic side to Asp96 (blue arrow) occurs during the transition from the N to N′ states. QM/MM-optimized structures of the (a) M and (b) N′ states with calculated $\nu_{C=O}$(Asp85). The black arrows indicate the C=O bond of Asp85. The blue label indicates the O...O distance between Asp85 and the adjacent water molecule (W603).

Asp85 is deprotonated[13,14,38] and Asp96 is protonated;[13−15,22] the Glu194/Glu204 pair shares one proton;[39] the retinal Schiff base has an *all-trans* form. During the transition from the J to K state, the retinal Schiff base is transformed into a twisted 13-*cis* form by photoisomerization.[40,41] Subsequently, it changes to a standard 13-*cis* form during the transition from the K to L

Table 3. Calculated pK_a, Distances of the O−H (r_{OH}) and C=O Bonds ($r_{C=O}$), the H-Bond Distance of O_{Asp85}-H···O_{H_2O} ($r_{O···O}$), and the Calculated and Observed $\nu_{C=O}$ Values for Asp85 in Bacteriorhodopsin

		calculation			experiment[a]		
state	Schiff base[b]	pK_a	r_{OH} (Å)	$r_{O···O}$ (Å)	$r_{C=O}$ (Å)	$\nu_{C=O}$ (cm^{-1})	$\nu_{C=O}$ (cm^{-1})
M	deprotonated	13.2	0.998	2.642	1.208	1827	1761
N′[c]	protonated	7.0	1.000	2.544	1.216	1785	1756

[a]Reference 15. [b]Protonation state of the retinal Schiff base. [c]The observed $\nu_{C=O}$ values of Asp85 in the N and N′ states were the same.[37]

state, removing the twist.[14,40,42] During the transition from the L to M state, two proton transfers (from the retinal Schiff base to Asp85[13−15] and from the Glu194/Glu204 pair to the extracellular side of the membrane[43,44]) occur. The proton transfers are followed by the next proton transfer from Asp96 to the retinal Schiff base during the transition from the M to N state.[13−15,37] The N state transitions to the N′ state with proton intake from the cytoplasmic side to Asp96.[14,22,37] During the transition from the N′ to the O state, the retinal Schiff base returns to the *all-trans* form from the *13-cis* form. Finally, the O state moves to the initial BR state, accompanied by proton transfer from Asp85 to the Glu194/Glu204 pair.[13−15,43] Here, we focus on the M and N′ intermediate states (Figure 7a).

The V49A mutant has been used as a model system for the N state in bacteriorhodopsin because it has a longer lifetime in the N and N′ states than the wild type. An FTIR study showed that the $\nu_{C=O}$ values of Asp85 in both the N and N′ states of the V49A mutant were the same as that in the N state of the wild type.[37] In this study, the N′ state structure of the V49A mutant was used as a model structure of the N state of the wild type by assuming that $\nu_{C=O}$ and pK_a of the wild type are similar to the N′ state of the V49A mutant.

By use of the electrostatic method, pK_a(Asp85) was calculated to be 13.2 (Table 3), which is consistent with the value of >11 estimated by FTIR analysis.[44] In contrast, it was calculated to be 7.0 in the N′ state. The calculated vibrational frequency of the C=O stretching bond of protonated Asp85 [$\nu_{C=O}$(Asp85)] thus shows a downshift of 42 cm^{-1} in the transition from the M (1827 cm^{-1}) to the N′ (1785 cm^{-1}) states (Figure 7 and Table 3), which is qualitatively consistent with the observed downshift of 7 cm^{-1} from the M (1761 cm^{-1}) to the N (1756 cm^{-1}) states.[15] These results indicate that the tendency of the correlation between $\nu_{C=O}$ and pK_a (i.e., the positive correlation) is the same as that observed in acetic acids. The calculated downshift of 42 cm^{-1} is quantitatively overestimated with respect to the experimental downshift of 7 cm^{-1}. This might be because of (1) the uncertainty of X-ray crystal structures and (2) a difference in the H-bond structure between the M and N′ structures. Note that the calculated frequency in the protein environment is highly sensitive to the H-bond structure as demonstrated in the calculation of the O−D stretching frequency of water molecules in bacteriorhodopsin.[39] A quantitative investigation of the relationship between $\nu_{C=O}$ and pK_a using an identical structure will be needed in the future.

The QM/MM-optimized geometry shows that the O−H bond distance, r_{OH}, in the N′ state is longer than that in the M state, whereas the C=O bond distance, $r_{C=O}$, in the N′ state is shorter than that in the M state (Table 3). The O−O distance, $r_{O···O}$, of the H-bond between Asp85 and the adjacent water molecule (W603) is shortened during the transition from the M to N′ states because pK_a(Asp85) decreases. These

tendencies are the same as those in acetic acids and can be explained by a similar scheme (Figure 8): Asp has no C=C
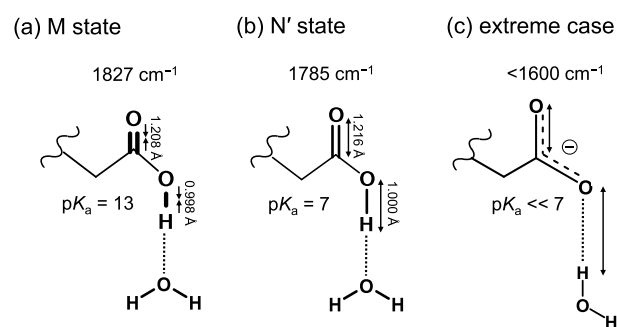

Figure 8. Correlation between r_{OH} and $r_{C=O}$ of Asp85 in bacteriorhodopsin: (a) M state and (b) N′ state. The calculated values of $\nu_{C=O}$, r_{OH}, and $r_{C=O}$ are shown. (c) Extreme case wherein Asp85 is deprotonated, i.e., pK_a(Asp85) ≪ 7.

bonds conjugated with the carboxylic group. As the proton leaves the donor O atom, the resonance effect between the C=O and C−O bonds in the carboxylic group becomes more pronounced, which weakens the double-bond nature of the C=O bond. Thereafter, the C=O bond strength is weakened, resulting in a longer $r_{C=O}$ than the typical C=O bond distance (Figure 8a−c).

The lower pK_a(Asp85) value (=7.0) in the N′ state than that in the M state (=13.2) is rationalized by the following: (i) because Asp85 is protonated in the N′ state, the pK_a(Asp85) value should not be less than 7, and (ii) as the Schiff base is also protonated in the N′ state, the pK_a(Asp85) value should decrease from that in the M state because of the repulsive interaction with the positive charge of the protonated Schiff base (Figure 7c). Thus, a decrease in the $\nu_{C=O}$ of Asp85 observed in bacteriorhodopsin during the transition from the M to N′ (N) state is attributable to a decrease in the pK_a of Asp85. Braiman et al. tried to explain the downshift as being caused by a local structural alteration of the C helix, which affects the environment of Asp85 in the transition from the M to N′ (N) states.[11] However, no significant structural change was observed in the C helix in the crystal structure of the N′ state reported later[22] compared with that of the M state[45] (Figure S5). The downshift of $\nu_{C=O}$ observed in bacteriorhodopsin during the transition from the M to N′ (N) state can be explained by the decrease in pK_a(Asp85) without invoking the structural change effect of the C helix.

Carboxylic Acids. The findings of this study can be extended to general saturated or unsaturated carboxylic acids. When the carboxylic acid has a C=C bond with the carboxylic group (i.e., unsaturated carboxylic acids), a negative correlation exists between pK_a and $\nu_{C=O}$ (Figure 9b). In contrast, when carboxylic acid has no conjugated C=C bond (i.e., saturated carboxylic acids), a positive correlation exists (Figure 9a). Note
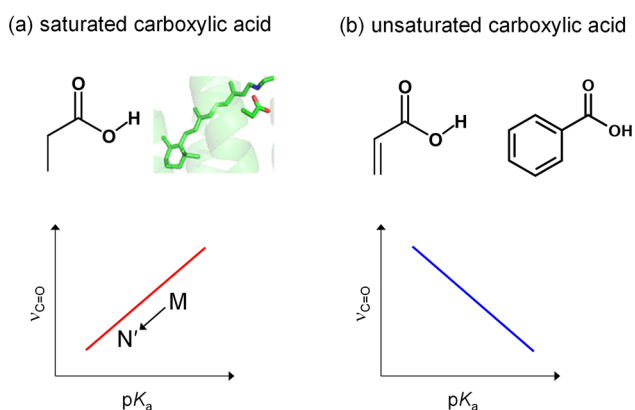
Figure 9. Schematic image of the correlation between pK_a and $\nu_{C=O}$: (a) saturated carboxylic acids (e.g., Asp); (b) unsaturated carboxylic acids (e.g., benzoic acids).

that these correlations cannot be used when the H-bond structures are not identical. Indeed, the slope and intercept of the fitting line depend on the number of water molecules H-bonded with the carboxylic group (Figure S3), although this tendency does not depend on it.

The pK_a shift of Asp and Glu in proteins was estimated from the negative correlation derived from benzoic acids[8,10] (e.g., in discussions on Asp85[11] and Asp96[12] in bacteriorhodopsin). These estimations should be revisited by using the positive correlation derived in this study, which may lead to completely opposite conclusions, as demonstrated here for bacteriorhodopsin.

CONCLUSIONS

The $\nu_{C=O}$ value of acetic acids increases as pK_a decreases (Figure 3a), whereas in benzoic acids, $\nu_{C=O}$ decreases as pK_a decreases (Figure 3c). The correlation between pK_a and $\nu_{C=O}$ depends on the presence or absence of the C=C double bond conjugated with the carboxylic group (Figures 5 and 6). These findings can be extended to general saturated or unsaturated carboxylic acids: the pK_a and $\nu_{C=O}$ values of saturated carboxylic acids (e.g., acetic acids) shows a positive correlation, whereas these two parameters shows a negative correlation in unsaturated carboxylic acids (e.g., benzoic acids) (Figure 9). This relationship can be applied to Asp or Glu in proteins as long as the structure of the H-bond network around the acid is identical, as shown by using the QM/MM calculations for bacteriorhodopsin (Table 3 and Figure 7). The previous discussions about Asp and Glu in proteins should therefore be revisited by using the positive correlation derived in this study instead of the well-established negative correlation derived from benzoic acids.[8,10]

ASSOCIATED CONTENT

ⓈI Supporting Information

The Supporting Information is available free of charge at https://pubs.acs.org/doi/10.1021/acs.jpcb.2c02193.

Figures and Tables; chemical structure of hydroxycarboxylic acid analogues; correlation between the measured pK_a and the calculated $\nu_{C=O}$, and the calculated C=O bond distances of hydroxycarboxylic acids; dependence of the correlation between the measured pK_a and the calculated $\nu_{C=O}$ on the number of H bonds; superimposed structure the N′ and M intermediate states; series of hydroxycarboxylic acids (PDF)

AUTHOR INFORMATION

Corresponding Authors

Keisuke Saito − *Department of Applied Chemistry, The University of Tokyo, Tokyo 113-8654, Japan; Research Center for Advanced Science and Technology, The University of Tokyo, Tokyo 153-8904, Japan;* ⓞ orcid.org/0000-0002-2293-9743; Phone: +81-3-5452-5056; Email: ksaito@appchem.t.u-tokyo.ac.jp; Fax: +81-3-5452-5083

Hiroshi Ishikita − *Department of Applied Chemistry, The University of Tokyo, Tokyo 113-8654, Japan; Research Center for Advanced Science and Technology, The University of Tokyo, Tokyo 153-8904, Japan;* ⓞ orcid.org/0000-0002-5849-8150; Email: hiro@appchem.t.u-tokyo.ac.jp

Author

Tianyang Xu − *Department of Applied Chemistry, The University of Tokyo, Tokyo 113-8654, Japan*

Complete contact information is available at: https://pubs.acs.org/10.1021/acs.jpcb.2c02193

Notes

The authors declare no competing financial interest.

REFERENCES

(1) Maeda, A.; Sasaki, J.; Shichida, Y.; Yoshizawa, T.; Chang, M.; Ni, B. F.; Needleman, R.; Lanyi, J. K. Structures of Aspartic Acid-96 in the L-Intermediate and N-Intermediate of Bacteriorhodopsin - Analysis by Fourier-Transform Infrared-Spectroscopy. *Biochemistry* **1992**, *31*, 4684−4690.

(2) Nabedryk, E.; Breton, J.; Hienerwadel, R.; Fogel, C.; Mantele, W.; Paddock, M. L.; Okamura, M. Y. Fourier-Transform Infrared Difference Spectroscopy of Secondary Quinone Acceptor Photoreduction in Proton-Transfer Mutants of Rhodobacter-Sphaeroides. *Biochemistry* **1995**, *34*, 14722−14732.

(3) Imamoto, Y.; Mihara, K.; Hisatomi, O.; Kataoka, M.; Tokunaga, F.; Bojkova, N.; Yoshihara, K. Evidence for Proton Transfer from Glu-46 to the Chromophore During the Photocyle of Photoactive Yellow Protein. *J. Biol. Chem.* **1997**, *272*, 12905−12908.

(4) Paddock, M. L.; Feher, G.; Okamura, M. Y. Identification of the Proton Pathway in Bacterial Reaction Centers: Replacement of Asp-M17 and Asp-L210 with Asn Reduces the Proton Transfer Rate in the Presence of Cd^{2+}. *Proc. Natl. Acad. Sci. U. S. A.* **2000**, *97*, 1548−1553.

(5) Sugo, Y.; Saito, K.; Ishikita, H. Mechanism of the Formation of Proton Transfer Pathways in Photosynthetic Reaction Centers. *Proc. Natl. Acad. Sci. U. S. A.* **2021**, DOI: 10.1073/pnas.2103203118.

(6) Kuroda, H.; Kawashima, K.; Ueda, K.; Ikeda, T.; Saito, K.; Ninomiya, R.; Hida, C.; Takahashi, Y.; Ishikita, H. Proton Transfer Pathway from the Oxygen-Evolving Complex in Photosystem Ii Substantiated by Extensive Mutagenesis. *Biochim. Biophys. Acta. Bioenerg.* **2021**, *1862*, 148329.

(7) Cao, Y.; Varo, G.; Klinger, A. L.; Czajkowsky, D. M.; Braiman, M. S.; Needleman, R.; Lanyi, J. K. Proton Transfer from Asp-96 to the Bacteriorhodopsin Schiff Base Is Caused by a Decrease of the Pka of Asp-96 Which Follows a Protein Backbone Conformational Change. *Biochemistry* **1993**, *32*, 1981−1990.

(8) Bellamy, L. J. *The Infrared Spectra of Complex Molecules: Advances in Infrared Group Frequencies*; Chapman & Hall: London, 1968; Vol. 2.

(9) Hay, M. B.; Myneni, S. C. B. Structural Environments of Carboxyl Groups in Natural Organic Molecules from Terrestrial Systems. Part 1: Infrared Spectroscopy. *Geochim. Cosmochim. Acta* **2007**, *71*, 3518−3532.

(10) Peltier, D.; Pichevin, A.; Dizabo, P.; Josien, M. L. Frequences De Valence Du Groupement Carbonyle Dune Serie Dacides Et Desters Benzoiques Monosubstitues Et Disubstitues - Relation Avec Le Pk Des Acides. *Comptes Rendus Hebdomadaires Des. Seances De L Academie Des. Sciences* **1959**, *248*, 1148−1150.

(11) Braiman, M. S.; Bousche, O.; Rothschild, K. J. Protein Dynamics in the Bacteriorhodopsin Photocycle - Submillisecond Fourier-Transform Infrared-Spectra of the L-Photointermediates, M-Photointermediates, and N-Photointermediates. *Proc. Natl. Acad. Sci. U. S. A.* **1991**, *88*, 2388−2392.

(12) Rothschild, K. J.; He, Y. W.; Sonar, S.; Marti, T.; Khorana, H. G. Vibrational Spectroscopy of Bacteriorhodopsin Mutants - Evidence That Thr-46 and Thr-89 Form Part of a Transient Network of Hydrogen-Bonds. *J. Biol. Chem.* **1992**, *267*, 1615−1622.

(13) Kandori, H. Hydration Switch Model for the Proton Transfer in the Schiff Base Region of Bacteriorhodopsin. *BBA-Bioenergetics* **2004**, *1658*, 72−79.

(14) Lanyi, J. K. Bacteriorhodopsin. *Annu. Rev. Physiol.* **2004**, *66*, 665−688.

(15) Radu, I.; Schleeger, M.; Bolwien, C.; Heberle, J. Time-Resolved Methods in Biophysics. 10. Time-Resolved FT-IR Difference Spectroscopy and the Application to Membrane Proteins. *Photoch Photobio Sci.* **2009**, *8*, 1517−1528.

(16) Cabaniss, S. E.; McVey, I. F. Aqueous Infrared Carboxylate Absorbances: Aliphatic Monocarboxylates. *Spectrochim Acta A* **1995**, *51*, 2385−2395.

(17) Nie, B. N.; Stutzman, J.; Xie, A. H. A Vibrational Spectral Maker for Probing the Hydrogen-Bonding Status of Protonated Asp and Glu Residues. *Biophys. J.* **2005**, *88*, 2833−2847.

(18) Takei, K.; Takahashi, R.; Noguchi, T. Correlation between the Hydrogen-Bond Structures and the C=O Stretching Frequencies of Carboxylic Acids as Studied by Density Functional Theory Calculations: Theoretical Basis for Interpretation of Infrared Bands of Carboxylic Groups in Proteins. *J. Phys. Chem. B* **2008**, *112*, 6725−6731.

(19) Gao, Q.; Leung, K. T. Hydrogen-Bonding Interactions in Acetic Acid Monohydrates and Dihydrates by Density-Functional Theory Calculations. *J. Chem. Phys.* **2005**, *123*, 074325.

(20) Brooks, C. J. W.; Eglinton, G.; Morman, J. F. Infrared spectra of aryl carboxylic acids and their esters. *J. Chem. Soc.* **1961**, 106−116.

(21) Jaguar Schrödinger, LLC, ver. 7.9: New York, 2012.

(22) Schobert, B.; Brown, L. S.; Lanyi, J. K. Crystallographic Intermediates of Structures of the M and N Bacteriorhodopsin: Assembly of a Hydrogen-Bonded Chain of Water Molecules between Asp-96 and the Retinal Schiff Base. *J. Mol. Biol.* **2003**, *330*, 553−570.

(23) Brooks, B. R.; Bruccoleri, R. E.; Olafson, B. D.; States, D. J.; Swaminathan, S.; Karplus, M. Charmm: A Program for Macromolecular Energy Minimization and Dynamics Calculations. *J. Comput. Chem.* **1983**, *4*, 187−217.

(24) QSite Schrödinger, LLC, ver. 5.8: New York, 2012.

(25) Scott, A. P.; Radom, L. Harmonic Vibrational Frequencies: An Evaluation of Hartree-Fock, Møller-Plesset, Quadratic Configuration Interaction, Density Functional Theory, and Semiempirical Scale Factors. *J. Phys. Chem.* **1996**, *100*, 16502−16513.

(26) Bashford, D.; Karplus, M. pK_a's of Ionizable Groups in Proteins: Atomic Detail from a Continuum Electrostatic Model. *Biochemistry* **1990**, *29*, 10219−10225.

(27) Nozaki, Y.; Tanford, C. Acid-Base Titrations in Concentrated Guanidine Hydrochloride. Dissociation Constants of Guanidinium Ion and of Some Amino Acids. *J. Am. Chem. Soc.* **1967**, *89*, 736−742.

(28) Baasov, T.; Sheves, M. Alteration of pK_a of the Bacteriorhodopsin Protonated Schiff Base. A Study with Model Compounds. *Biochemistry* **1986**, *25*, 5249−5258.

(29) Rousso, I.; Friedman, N.; Sheves, M.; Ottolenghi, M. pK_a of the Protonated Schiff-Base and Aspartic-85 in the Bacteriorhodopsin Binding-Site Is Controlled by a Specific Geometry between the 2 Residues. *Biochemistry* **1995**, *34*, 12059−12065.

(30) Tanokura, M. ¹H-NMR Study on the Tautomerism of the Imidazole Ring of Histidine Residues. I. Microscopic Pk Values and Molar Ratios of Tautomers in Histidine-Containing Peptides. *Biochim. Biophys. Acta* **1983**, *742*, 576−85.

(31) Tanokura, M. ¹H-NMR Study on the Tautomerism of the Imidazole Ring of Histidine Residues. II. Microenvironments of Histidine-12 and Histidine-119 of Bovine Pancreatic Ribonuclease A. *Biochim. Biophys. Acta* **1983**, *742*, 586−96.

(32) Tanokura, M. 1h Nuclear Magnetic Resonance Titration Curves and Microenvironments of Aromatic Residues in Bovine Pancreatic Ribonuclease A. *J. Biochem* **1983**, *94*, 51−62.

(33) Rabenstein, B.; Knapp, E. W. Calculated pH-Dependent Population and Protonation of Carbon-Monoxy-Myoglobin Conformers. *Biophys. J.* **2001**, *80*, 1141−1150.

(34) Dean, J. A. *Lange's Handbook of Chemistry*; McGraw-Hill, Inc.: New York, 1999.

(35) Han, J.; Deming, R. L.; Tao, F. M. Theoretical Study of Hydrogen-Bonded Complexes of Chlorophenols with Water or Ammonia: Correlations and Predictions of pK_a Values. *J. Phys. Chem. A* **2005**, *109*, 1159−1167.

(36) Ishikita, H.; Saito, K. Proton Transfer Reactions and Hydrogen-Bond Networks in Protein Environments. *J. R Soc. Interface* **2014**, *11*, 20130518.

(37) Dioumaev, A. K.; Brown, L. S.; Needleman, R.; Lanyi, J. K. Coupling of the Reisomerization of the Retinal, Proton Uptake, and Reprotonation of Asp-96 in the N Photointermediate of Bacteriorhodopsin. *Biochemistry* **2001**, *40*, 11308−11317.

(38) Rouhani, S.; Cartailler, J. P.; Facciotti, M. T.; Walian, P.; Needleman, R.; Lanyi, J. K.; Glaeser, R. M.; Luecke, H. Crystal Structure of the D85s Mutant of Bacteriorhodopsin: Model of an O-Like Photocycle Intermediate. *J. Mol. Biol.* **2001**, *313*, 615−28.

(39) Saito, S.; Kandori, H.; Ishikita, H. Factors That Differentiate the H-Bond Strengths of Water near the Schiff Bases in Bacteriorhodopsin and *Anabaena* Sensory Rhodopsin. *J. Biol. Chem.* **2012**, *287*, 34009−18.

(40) Nogly, P. Retinal Isomerization in Bacteriorhodopsin Captured by a Femtosecond X-Ray Laser. *Science* **2018**, DOI: 10.1126/science.aat0094.

(41) Kovacs, G. N., et al. Three-Dimensional View of Ultrafast Dynamics in Photoexcited Bacteriorhodopsin. *Nat. Commun.* **2019**, *10*.

(42) Miller, R. J. D.; Pare-Labrosse, O.; Sarracini, A.; Besaw, J. E. Three-Dimensional View of Ultrafast Dynamics in Photoexcited Bacteriorhodopsin in the Multiphoton Regime and Biological Relevance. *Nat. Commun.* **2020**.

(43) Balashov, S. P. Protonation Reactions and Their Coupling in Bacteriorhodopsin. *Biochim. Biophys. Acta* **2000**, *1460*, 75−94.

(44) Braiman, M. S.; Dioumaev, A. K.; Lewis, J. R. A Large Photolysis-Induced pK_a Increase of the Chromophore Counterion in Bacteriorhodopsin: Implications for Ion Transport Mechanisms of Retinal Proteins. *Biophys. J.* **1996**, *70*, 939−947.

(45) Takeda, K.; Matsui, Y.; Kamiya, N.; Adachi, S.; Okumura, H.; Kouyama, T. Crystal Structure of the M Intermediate of Bacteriorhodopsin: Allosteric Structural Changes Mediated by Sliding Movement of a Transmembrane Helix. *J. Mol. Biol.* **2004**, *341*, 1023−1037.